

## PDF hosted at the Radboud Repository of the Radboud University Nijmegen

The following full text is a publisher's version.

For additional information about this publication click this link.

<http://hdl.handle.net/2066/178035>

Please be advised that this information was generated on 2018-07-07 and may be subject to change.

## Umbilical cord blood CD34<sup>+</sup> progenitor-derived NK cells efficiently kill ovarian cancer spheroids and intraperitoneal tumors in NOD/SCID/IL2Rg<sup>null</sup> mice

Janneke S. Hoogstad-van Evert, Jeannette Cany, Dirk van den Brand, Manon Oudenampsen, Roland Brock, Ruurd Torensma, Ruud L. Bekkers, Joop H. Jansen, Leon F. Massuger & Harry Dolstra

To cite this article: Janneke S. Hoogstad-van Evert, Jeannette Cany, Dirk van den Brand, Manon Oudenampsen, Roland Brock, Ruurd Torensma, Ruud L. Bekkers, Joop H. Jansen, Leon F. Massuger & Harry Dolstra (2017) Umbilical cord blood CD34<sup>+</sup> progenitor-derived NK cells efficiently kill ovarian cancer spheroids and intraperitoneal tumors in NOD/SCID/IL2Rg<sup>null</sup> mice, *Oncolimmunology*, 6:8, e1320630, DOI: [10.1080/2162402X.2017.1320630](https://doi.org/10.1080/2162402X.2017.1320630)

To link to this article: <https://doi.org/10.1080/2162402X.2017.1320630>



© 2017 The Author(s). Published with license by Taylor & Francis Group, LLC© Janneke S. Hoogstad-van Evert, Jeannette Cany, Dirk van den Brand, Manon Oudenampsen, Roland Brock, Ruurd Torensma, Ruud L. Bekkers, Joop H. Jansen, Leon F. Massuger and Harry Dolstra



[View supplementary material](#)



Accepted author version posted online: 11 May 2017.  
Published online: 03 Aug 2017.



[Submit your article to this journal](#)



Article views: 795



[View related articles](#)



[View Crossmark data](#)



Citing articles: 2 [View citing articles](#)

ORIGINAL RESEARCH



## Umbilical cord blood CD34<sup>+</sup> progenitor-derived NK cells efficiently kill ovarian cancer spheroids and intraperitoneal tumors in NOD/SCID/IL2Rg<sup>null</sup> mice

Janneke S. Hoogstad-van Evert<sup>a,b</sup>, Jeannette Cany<sup>a</sup>, Dirk van den Brand<sup>c</sup>, Manon Oudenampsen<sup>a</sup>, Roland Brock<sup>c</sup>, Ruud Torensma<sup>d</sup>, Ruud L. Bekkers<sup>b</sup>, Joop H. Jansen<sup>a</sup>, Leon F. Massuger<sup>b</sup>, and Harry Dolstra<sup>a</sup>

<sup>a</sup>Department of Laboratory Medicine, Laboratory of Hematology, Radboud University Medical Center, Nijmegen, the Netherlands; <sup>b</sup>Department of Obstetrics and Gynecology, Radboud University Medical Center, Nijmegen, the Netherlands; <sup>c</sup>Department of Biochemistry, Radboud University Medical Center, Nijmegen, the Netherlands; <sup>d</sup>Department of Tumor Immunology, Radboud University Medical Center, Nijmegen, the Netherlands

### Key Points

1. HSPC-NK cells efficiently destruct ovarian carcinoma spheroids *in vitro* and target intraperitoneal ovarian tumors *in vivo*.
2. HSPC-NK cells actively migrate, infiltrate and mediate intratumoral cell killing in a three-dimensional ovarian cancer spheroid.

### ABSTRACT

Adoptive transfer of allogeneic natural killer (NK) cells is an attractive therapy approach against ovarian carcinoma. Here, we evaluated the potency of highly active NK cells derived from human CD34<sup>+</sup> haematopoietic stem and progenitor cells (HSPC) to infiltrate and mediate killing of human ovarian cancer spheroids using an *in vivo*-like model system and mouse xenograft model. These CD56<sup>+</sup>Perforin<sup>+</sup> HSPC-NK cells were generated under stroma-free conditions in the presence of StemRegenin-1, IL-15, and IL-12, and exerted efficient cytolytic activity and IFN $\gamma$  production toward ovarian cancer monolayer cultures. Live-imaging confocal microscopy demonstrated that these HSPC-NK cells actively migrate, infiltrate, and mediate tumor cell killing in a three-dimensional multicellular ovarian cancer spheroid. Infiltration of up to 30% of total HSPC-NK cells within 8 h resulted in robust tumor spheroid destruction. Furthermore, intraperitoneal HSPC-NK cell infusions in NOD/SCID-IL2R $\gamma$ <sup>null</sup> (NSG) mice bearing ovarian carcinoma significantly reduced tumor progression. These findings demonstrate that highly functional HSPC-NK cells efficiently destruct ovarian carcinoma spheroids *in vitro* and kill intraperitoneal ovarian tumors *in vivo*, providing great promise for effective immunotherapy through intraperitoneal HSPC-NK cell adoptive transfer in ovarian carcinoma patients.

### ARTICLE HISTORY

Received 17 January 2017  
Revised 11 April 2017  
Accepted 13 April 2017

### KEYWORDS

Adoptive immunotherapy;  
mouse ovarian cancer  
xenograft; NK cells; ovarian  
cancer; tumor spheroid  
infiltration


## Introduction

Ovarian cancer (OC) is the fifth leading cause of cancer-related death in women.<sup>1</sup> Since patients with early-stage OC seldom have clinical symptoms, most patients are diagnosed at advanced stage with peritoneal tumor dissemination and ascites. Standard treatment of OC patients is cytoreductive surgery combined with platinum/taxane chemotherapy. Although OC is sensitive to chemotherapy, the 5-y survival is 46% for all stages of OC, and only 20% and 6% for advanced stage III and IV disease,<sup>1</sup> respectively. In the last decades, only slight improvements have been made to increase patient outcomes, so there is an unmet need for novel therapeutic strategies as most women with relapsed or metastatic OC ultimately die of progressive disease.

Adoptive cell therapy (ACT) exploiting allogeneic natural killer (NK) cells could be a novel, relatively non-toxic, and attractive treatment approach against OC. In particular, intraperitoneal (i.p.) infusion, rather than intravenous (i.v.)

administration, of pre-activated or expanded NK cells is a promising strategy to better control ovarian tumors confined to the peritoneal cavity.<sup>2, 3</sup> However, effective ACT requires NK cells to be appropriately activated, available in sufficient numbers, and have a good persistence *in vivo*.<sup>4</sup> Furthermore, effective NK cell infiltration into solid tumor tissue and tumor cell killing upon encounter is required. Generally, allogeneic NK cell products have been enriched from peripheral blood (PB) of haplo-identical donors followed by overnight activation with IL-2 or IL-15. However, this cellular product is rather heterogeneous with 25–95% of infused cells being NK cells depending on the used enrichment method and contains a variable number of monocytes, B cells, and potentially alloreactive T cells capable of inducing graft-versus-host disease.<sup>5–7</sup> Furthermore, this approach yields relatively low NK cell numbers, enough for only a single dose, while higher numbers and multiple dosing require further expansion before adoptive transfer.<sup>4</sup> For these reasons, development of more homogeneous, scalable and

**CONTACT** Janneke S. Hoogstad-van Evert  [Janneke.Hoogstad-vanEvert@Radboudumc.nl](mailto:Janneke.Hoogstad-vanEvert@Radboudumc.nl)  Department of Laboratory Medicine, Laboratory of Hematology, Radboudumc, Geert Grooteplein 8, P.O. Box 9101, 6500 HB, Nijmegen, the Netherlands.

 Supplemental data for this article can be accessed on the [publisher's website](#).

Published with license by Taylor & Francis Group, LLC © Janneke S. Hoogstad-van Evert, Jeannette Cany, Dirk van den Brand, Manon Oudenampsen, Roland Brock, Ruud Torensma, Ruud L. Bekkers, Joop H. Jansen, Leon F. Massuger and Harry Dolstra.

This is an Open Access article distributed under the terms of the Creative Commons Attribution-NonCommercial License (<http://creativecommons.org/licenses/by-nc/4.0/>), which permits unrestricted non-commercial use, distribution, and reproduction in any medium, provided the original work is properly cited.

“off-the-shelf” allogeneic NK cell products is preferable for adoptive immunotherapy.

Alternatively, NK cells can be generated *ex vivo* from haematopoietic stem and progenitor cells (HSPC) or induced pluripotent stem cells (iPSC).<sup>3,8-10</sup> Previously, we reported good manufacturing practice (GMP)-compliant, cytokine-based culture protocols for the *ex vivo* generation of highly active NK cells from CD34<sup>+</sup> HSPCs isolated from various stem cell sources.<sup>9-12</sup> By applying the aryl hydrocarbon receptor (AHR) antagonist StemRegenin-1 (SR1) and the combination of IL-15 and IL-12, we demonstrated that highly active CD56<sup>+</sup> NK cells can be generated with potent functional activity toward hematological tumor cells *in vitro* as well as anti-leukemic effects *in vivo* following i.v. administration.<sup>9,10,13</sup> In addition, we observed that these HSPC-NK cells efficiently kill melanoma cell lines<sup>12</sup> and renal cell carcinoma cell lines *in vitro* (unpublished), and therefore HSPC-NK cells are attractive for allogeneic NK cell ACT against refractory OC and other solid tumors.

Many studies, including ours, have shown that pre-activated or expanded NK cells rapidly recognize and destroy malignantly transformed cells *in vitro*.<sup>2,3,7,9,10,12-22</sup> However, the majority of reported studies is based on tumor cell monolayer culture systems neglecting the three-dimensional (3D) tumor structure, thereby allowing only limited translation to the *in vivo* situation. Therefore, 3D multicellular tumor spheroid models have been developed to better investigate infiltration and intra-tumoral cytotoxicity by NK cells.<sup>15,16,23</sup> Furthermore, adoptive transfer studies should be performed in relevant human OC xenograft models to study the optimal delivery route, *in vivo* persistence of function and potency of well-defined NK cell products. Recently, Hermanson et al. demonstrated in a mouse model with the OC cell line MA148 that i.p. delivery of iPSC-derived NK cells inhibits tumor growth at least as efficient as PB-enriched NK cells.<sup>3</sup> In the present study, we investigated the preclinical efficacy of *ex vivo* generated, highly functional HSPC-NK cells generated by a novel combined SR1/IL-15/IL-12-based culture protocol in clinically relevant OC models. Flow cytometry (FCM) analysis and live-imaging confocal microscopy demonstrate that these HSPC-NK cells efficiently infiltrate, migrate, and kill OC cells in 3D tumor spheroids. Moreover, we demonstrate that i.p. infusions of this HSPC-NK cell product mediate a potent anti-OC effect in an SKOV-3-based xenograft model and significantly prolong mice survival. These preclinical studies provide the rationale to pursue clinical trials using adoptive transfer of HSPC-NK cells in OC patients.

## Material and methods

### HSPC-NK cell generation

Umbilical cord blood (UCB) units were collected in CB-collect bags (Fresenius Kabi) at caesarean sections after full term pregnancy and informed consent was obtained of the mother (CMO 2014-226). CD34<sup>+</sup> HSPCs were isolated from mononuclear cells after Ficoll-Hypaque density-gradient centrifugation and CD34-positive immunomagnetic bead selection (Miltenyi Biotec, 130046702). After isolation, CD34<sup>+</sup> HSPCs were cryopreserved or directly used for NK cell generation. Cultures were performed for 6 weeks in six-well tissue culture plates

(Corning CLS3506), using CellGro DC medium (CellGenix 20801-0500) supplemented with 10% and 2% human serum (Sanquin Bloodbank) during the expansion and the differentiation phase, respectively. Cells were cultured using three successive cytokine cocktails, and in the presence of 2  $\mu$ M SR1 (Cellagen Technology, C7710-5) till day 21. In the first 9 d, CD34<sup>+</sup> HSPCs were expanded with 25 ng/mL IL-7, 25 ng/mL stem cell factor (SCF), 25 ng/mL Flt3L (all ImmunoTools, 11340077, 11343328, 11343307), and 25 ng/mL thrombopoietin (TPO; CellGenix, 1417-050). At day 9, TPO was replaced by 50 ng/mL IL-15 (ImmunoTools, 11343615). Thereafter, expanded cells were cultured in differentiation medium consisting of 20 ng/mL IL-7, 20 ng/mL SCF, 50 ng/mL IL-15, and 0.2 ng/mL IL-12 (Miltenyi Biotec, 130-096-704). Total cell number and CD56 acquisition were analyzed twice a week by flow cytometry, and medium was refreshed every 2 to 4 d to keep cell density between 1.5 and 2.5  $\times 10^6$  cells/mL. HSPC-NK cell products were used in experiments after 5 to 6 weeks of culture with >90% CD56+ cells.

### Patient samples

Patient material was obtained from stage III and IV OC patients before primary treatment in the Radboud University Medical Center (Radboudumc) after written informed consent. Fresh ascites was filtered using a 100  $\mu$ m filter, centrifuged, and resuspended in phosphate buffered saline (PBS). Subsequently, mononuclear cells were isolated using a Ficoll-Hypaque (1.077 g/mL; GE Healthcare, 17-1440-03) density gradient. Samples were cryopreserved in dimethyl sulfoxide (DMSO)-containing medium and used after thawing.

### Culture of OC cell lines

OC cell lines SKOV-3 and IGROV1 were cultured in Roswell Park Memorial Institute medium (RPMI 1640; Gibco, 11875119) with 10% Fetal Calf Serum (FCS; Integro). The OVCAR-3 cell line was cultured in RPMI 1640 medium with 20% FCS and 1  $\mu$ g/mL insulin (Sigma 10516). K562 cells were cultured in Iscove's Modified Dulbecco's medium (IMDM; Gibco, 21980065) containing 10% FCS. SKOV-3-GFP-luc cells were generated by stable transduction of parental cells with lentiviral particles LVP20 encoding the reporter genes green fluorescent protein (GFP) and luciferase (luc) under control of the CMV promoter (GenTarget, LVP020). Transduced cells were cloned and an optimal SKOV-3-GFP-luc clone for *in vitro* and *in vivo* experiments was selected based on GFP expression, luciferase activity, and comparable susceptibility to HSPC-NK killing as the parental cell line.

### Multicellular tumor spheroids

OC tumor spheroids were generated by seeding 3  $\times 10^4$  cells/well in a volume of 100  $\mu$ L/well of culture medium in 96-well plates coated with 1% agarose in DMEM/F12 medium (Invitrogen 11330-057) with 0.3% bovine serum albumin (Sigma Aldrich A3156), which is adjusted from Giannattasio et al. and nature protocols.<sup>15,24</sup> Tumor spheroids were used for functional assays upon reaching a solid state after 72 h after initial seeding.

### Flow cytometry (FCM)

HSPC-NK cell numbers and expression of cell surface markers were determined by FCM. Anti-CD45-ECD (Beckman Coulter, A07784) and anti-CD56-PC7 (BioLegend, 318318) antibodies were used to follow cell number and NK cell differentiation during culture using the Coulter FC500 flow cytometer (Beckman Coulter). The population of viable cells was determined by exclusion of 7-amino-actinomycin D (7-AAD) positive cells (Sigma A9400). For phenotypical analysis, cells were incubated with antibodies in FCM buffer (PBS/0.5% bovine serum albumin) for 30 min at 4°C. After washing, cells were resuspended in FCM buffer and analyzed. The following fluorochrome-conjugated monoclonal antibodies were used: CD3 A07748, CD14 325604, CD19 302228, CD56 318318, NKG2A A60797, NKp30 325208, NKp44 325108, NKp46 331908, NKG2D 320806, DNAM-1 559788, TRAIL 308210, CD69 310904, CD16 302006, KIR's 312606, CXCR3 353708, CD62L 304821, CD11a 301206, CD107a 328618, HLA-ABC 311410, HLA-E 342603, MIC A/B 320908, ULBP-1 FAB1380A, ULBP-2 FAB1298P, TRAIL-R1 307208, TRAIL-R2 307406, CD112 337410, and CD155 FAB25301A all Biolegend, R&D systems, e-bioscience or BD Biosciences.

The analysis of NK cell reactivity at the single cell level was determined following 4 h stimulation with K562 cells in the presence of anti-CD107a and Brefeldin A (555029 BD Biosciences) and subsequent intracellular staining for perforin (308106, Biolegend) and IFN $\gamma$  (554700 BD Biosciences) and EOMES (11-4877-41 e-bioscience). Flow cytometric analysis was performed with exclusion of dead cells with Fixable Viability Dye eFluor780 (65-0865-18 eBiosciences), gating on CD56<sup>+</sup>Perforin<sup>+</sup> NK cells, and using unstimulated cells as control.

### FCM-based cytotoxicity and infiltration assays

In monolayer cytotoxicity assays, tumor cells were first seeded at a concentration of  $3 \times 10^4$  in flat-bottom 96-well plates in triplicate for each test condition. The following day, HSPC-NK cells were labeled with 1  $\mu$ M carboxyfluorescein diacetate succinimidyl ester (CFSE; Invitrogen, C34554) and were added at different effector-to-target (E:T) ratios (1:1, 3:1 and 10:1). For cytotoxicity assays with SKOV-3-GFP cells, HSPC-NK cells were added without CFSE staining. After 24 h, co-culture supernatants were harvested and stored at -20°C until use for enzyme-linked immunosorbent assay (ELISA). Subsequently, cells in each well were gently resuspended and suspension cells were collected in Micronics tubes. Next, adherent cells were detached using trypsin, collected, and added to the tubes. Then, the life/dead marker 7-AAD was added to the cells and absolute numbers of viable targets present in each well were determined by FCM (FC500, Beckman Coulter). The specific killing of OC cells by NK cells was calculated with the following formula:  $1 - (\text{number of viable target cells after co-culture with NK cells} / \text{number of viable target cells cultured alone}) \times 100\%$ .

In cytotoxicity assays with OC spheroids, day 3 spheres were used as described previously by Giannattasio et al.<sup>15</sup> Again, HSPC-NK cells were added at different dosages  $2 \times 10^5$ ,  $6 \times$

$10^5$ ,  $2 \times 10^6$ /well. After 24 h of co-culture, supernatant of the  $2 \times 10^5$  NK cells was collected for ELISA. Spheroids were washed, and trypsinized and double negative target cells for CFSE and 7-AAD were counted using the FC500 flow cytometer.

In the co-culture supernatants, production of granzyme B (GzmB) and IFN $\gamma$  by HSPC-NK cells was evaluated by ELISA according to the manufacturer's instructions (IFN $\gamma$ ; Perbio Scientific M700A and GzmB; Mabtech, 3485-1H-20).

For the FCM-based infiltration assay, we performed the spheroid cytotoxicity assay as described above. Infiltrating vs. non-infiltrating HSPC-NK cells were collected separately as described previously by Giannattasio et al.<sup>15</sup> For this, after fixed time point, supernatant was first collected containing the non-infiltrated NK cells. Subsequently, remaining spheroids were washed twice, trypsinized, and transferred in separate tubes. In this cell suspension of the spheroid are the infiltrated NK cells. Absolute NK cell counts were determined by FCM for each well at different time points in supernatant (contains non-infiltrating HSPC-NK cells) and cell suspension after trypsinization (contains infiltrated HSPC-NK cells).

Intra-tumoral cytotoxicity of infiltrated HSPC-NK cells was determined by transferring HSPC-NK cell treated spheres after 5 h of co-culture to a new well, and subsequently determining the specific killing after overnight incubation.

### Confocal microscopic imaging of NK cell invasion and killing in multicellular spheroids

Co-culture of OC spheroids and HSPC-NK cells was performed as described above. For confocal experiments, SKOV-3-GFP cells were co-cultured with CD56-APC and GAM-AF647 labeled NK cells. After co-culture, spheres were collected, washed mildly with PBS/BSA buffer, and placed in an Ibidi  $\mu$ -slide eight-well plate (Ibidi, 80826) in RPMI without phenol red, and Propidium iodide (PI) (Sigma-Aldrich, 247-081-0) was added to a final concentration of 50  $\mu$ g/mL to detect cell death. Imaging was performed with a Leica TCS SP5 microscope (Leica Microsystems, Germany) at 37°C using an HC PL Fluotar 20.0  $\times$  0.5 dry lens. Laser power, gain and offset were kept constant between experiments and conditions. End point experiments were performed at 0, 1, 3, and 5 h and z-stacks of confocal sections were acquired with a step size of 5  $\mu$ m. Time lapse movies were made by imaging with a time interval of 30 s and a maximum acquisition time of ~5 h in a fixed z-plane. GFP and PtdIns were excited with the argon laser line at 488 nm and emission was detected between 495 and 550 nm for GFP and between 595 and 640 nm for PtdIns. In a sequential scan APC and GAM-AF647 were excited with the HeNe laser at 633 nm, and emission was measured between 640 nm and 710 nm.

### Image analysis

The acquired images were analyzed with Fiji image analysis software.<sup>25</sup> For qualitative representation, the brightness and contrast settings were adjusted for better visualization. The same settings were used for all images. Cell death was quantified by placing a threshold on the PtdIns channel and creating a binary image for every z-plane. Subsequently,

particles were separated by performing a dilute, erode, and watershed operation on the image. For every z-plane, a separate region-of-interest (ROI) was drawn around the edge of the spheroid, based on the image in the GFP channel. The area of each ROI was measured and the number of particles bigger than  $20 \mu\text{m}^2$  was counted. To correct for size differences between different z-planes and spheroids, the ratio between the number of particles and the measured area was used to represent cell death. Cell death in depth was measured on the 5h HSPC-NK cell co-culture spheroids, and the 250 min time lapse was used for the analysis of cell death in time and compared with time points in untreated spheres.

### **Adoptive transfer studies of HSPC-NK cells in intraperitoneal OC mouse model**

All experiments were approved by the Radboudumc animal care and user committee (DEC 2014-150). In the first experiment, 11 NOD/SCID/IL2Rg<sup>null</sup> mice (Jackson laboratories) of 6-12 week old were injected intraperitoneally (i.p.) with  $1.0 \times 10^6$  cells SKOV-3-GFP-Luc cells and divided randomly into two treatment groups (i.e., control vs. NK i.p.), after the first BLI at day 3. After 4 and 11 days, mice of the i.p. treatment group received two i.p. HSPC-NK cell infusions ( $12 \times 10^6$  cells/mouse/infusion). In addition treated mice received  $1 \mu\text{g}$  recombinant human IL-15 (Immunotools, 11340158) subcutaneously every 48 h till day 21. Bioluminescence images were collected weekly till day 56. For this, mice were injected i.p. with D-luciferin 150 mg/kg (PerkinElmer 122796), after 10 min anesthetized with isoflurane and bioluminescence images were collected in the IVIS using the Living Image processing software. ROI were drawn around the abdominal area of the mice, and measurements were automatically generated as integrated flux of photons (photons/s). The second experiment was performed with a lower tumor dose of  $0.2 \times 10^6$  SKOV-3-GFP-Luc cells and again two infusions of  $12 \times 10^6$  HSPC-NK cells were given. Bioluminescence images were collected weekly till day 56. Blood collection was performed till day 35 by tail puncture. After erylisis, the flowcytometric analysis of human CD45+ cells vs. mouse CD45 cells was performed to calculate the percentage of human CD56+ cells. All mice were followed till day 92 for survival. Following euthanasia, a macroscopic tumor score was given by two independent researchers using the following classification: 0 for no macroscopic tumor, 1 for small tumors  $<5$  mm and 2 for large tumors  $\geq 5$  mm. From paraffin-embedded samples,  $5\text{-}\mu\text{m}$  tissue sections were cut and placed on polylysine-coated glass slides for immunohistochemistry. The method described by Taylor et al. was used for Ki67 staining.<sup>26</sup>

### **Statistics**

Data analysis was conducted by Prism software (GraphPad, version 5.03 for Windows). Two-way ANOVA or Student *t*-test was used to calculate statistically significant differences between groups. The survival probability was estimated by the Kaplan–Meier methods, and *p*-value was calculated with a log-

rank Mantel–Cox test. A *p*-value of  $< 0.05$  was considered statistically significant.

## **Results**

### **Ex vivo generation of highly functional HSPC-NK cells**

We showed recently that inhibition of the AHR using SR1 improves NK cell generation from CD34<sup>+</sup> HSPCs by enhancing the expression level of several transcription factors involved in early NK cell development.<sup>10</sup> In addition, we reported that combining IL-15 with IL-12 drives the differentiation of more mature and highly functional HSPC-NK cells, which display potent alloreactivity toward haematological cancer cells.<sup>9</sup> In the present study, we combined SR1, IL-15, and IL-12 to generate HSPC-NK cells and test their tumor-reactivity against OC. As illustrated in Fig. 1, this culture protocol resulted in  $>1,000$ -fold expansion and differentiation into  $>80\%$  CD45<sup>+</sup>CD56<sup>+</sup>CD3<sup>-</sup> cells before washing, after washing even  $>90\%$  (Fig. 1A and Table S1). Non-CD56<sup>+</sup> cells present in the final product were comprised of CD14<sup>+</sup> myeloid cells and  $<0.05\%$  CD19<sup>+</sup> B cells (Fig. 1B). Contaminating T cells were virtually absent ( $< 0.05\%$ ). After 6 weeks of culture, NK cell yields were determined using CD56 and NKG2A markers, which discriminated between conventional EOMES<sup>+</sup>Perforin<sup>+</sup> NK cells and other innate lymphoid cells (Fig. 1B). On average, the SR1/IL-15/IL-12 culture protocol yielded  $1,097 \times 10^6$  CD56+ cells calculated from  $1 \times 10^6$  CD34<sup>+</sup> cells (range 833–1,843,  $n = 7$ , Table S1). These cells displayed a high expression level of activating receptors (Fig. 1C). The expression profile of other maturation markers, as well as homing and adhesion molecules was similar to that previously reported on HSPC-NK cell products generated either in the presence of SR1 or IL-15/IL-12 combination.<sup>9,10</sup> Furthermore, these novel SR1/IL-15/IL-12-induced HSPC-NK cells demonstrated high cytolytic activity and IFN $\gamma$  production capacity against K562 cells at low E:T ratios (Fig. 1D). Potent NK cell activation and reactivity was further confirmed at the single cell level with induction of significant proportions of degranulating CD107a<sup>+</sup> and IFN $\gamma$ <sup>+</sup> NK cells upon short-term stimulation (Fig. 1E). These data show that SR1/IL-15/IL-12-induced HSPC-NK cells can be generated at high numbers and are highly functional, providing a strong rationale for HSPC-NK-cell based immunotherapy.

### **HSPC-NK cells efficiently kill ovarian carcinoma cells**

To explore the potential of HSPC-NK cells against OC, we first performed cytotoxicity assays with several frequently used OC cell lines (SKOV-3, IGROV1, and OVCAR-3). The NK-sensitive K562 cells were included as a positive control. At an E:T ratio of 1:1, 24–79% killing was observed after overnight co-culture (Fig. 2A). This was increased to  $>90\%$  using higher E:T ratios and potent killing capacity was seen for all used HSPC-NK cell products that were generated from different UCB donors. To further demonstrate high reactivity of HSPC-NK cells toward OC cells, ELISA for IFN $\gamma$  and GzmB were performed on co-culture supernatants.

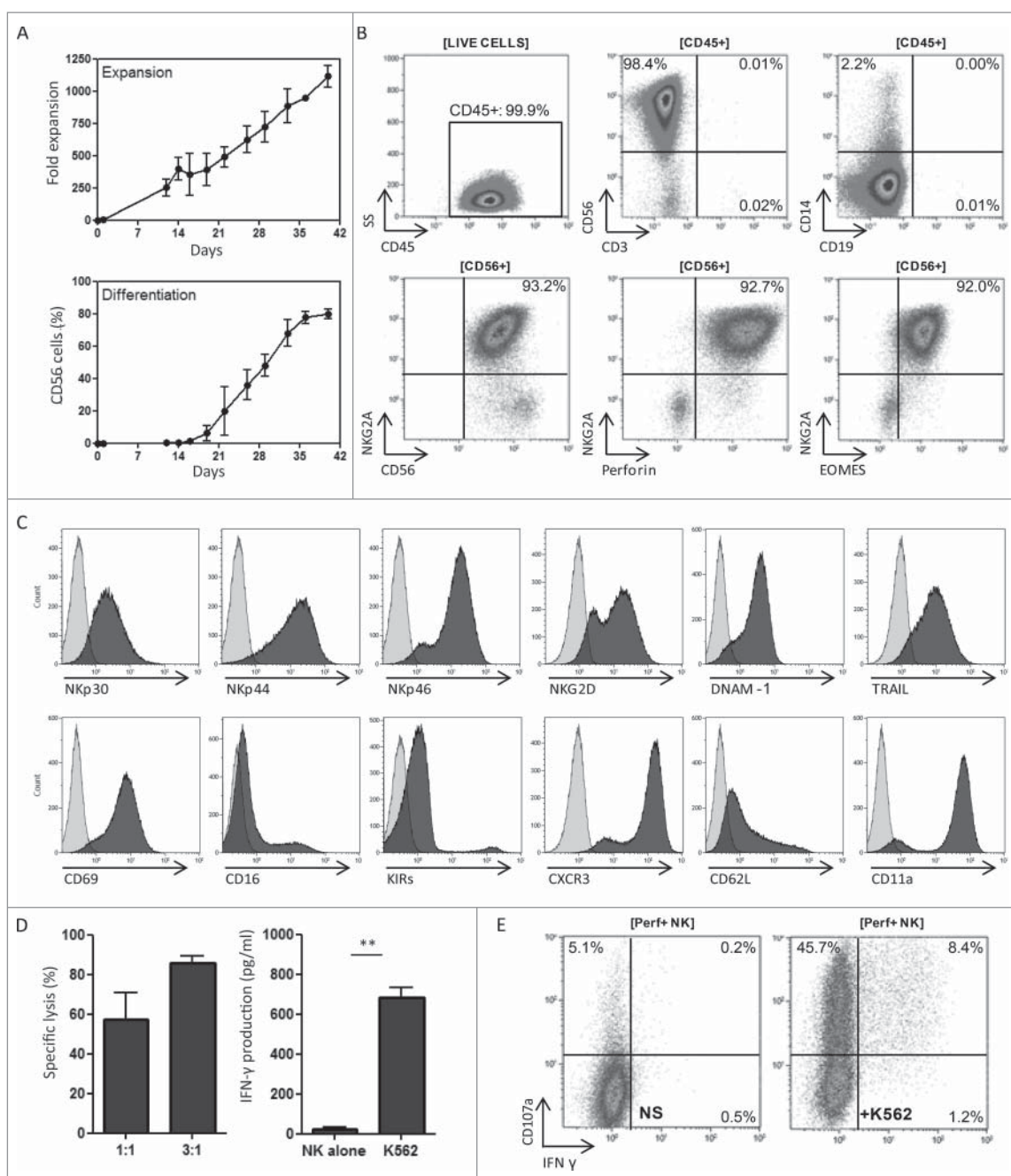


**Figure 1.** SR1/IL-15/IL-12-induced HSPC-NK cells can be generated at high numbers and are highly functional. (A) Fold expansion of seven HSPC-NK cell products cultured for 40 d depicted as the mean with SD in the upper half. In the lower half, the percentage of CD56<sup>+</sup> cells counted by flow cytometry is depicted as the mean with SD. (B) Representative FCM dot plots of an SR1/IL-15/IL-12-generated HSPC-NK cell product with high frequency of CD56<sup>+</sup>, NKG2A<sup>+</sup>, perforin<sup>+</sup>, and EOMES<sup>+</sup> conventional NK cells. (C) Histograms illustrating the high expression level of activating receptors on SR1/IL-15/IL-12 generated HSPC-NK cell products. (D) SR1/IL-15/IL-12-induced HSPC-NK cells demonstrated high cytolytic activity (left figure) and IFN $\gamma$  production (right figure) against K562 cells at a low E:T ratio of 1:1, *t*-test 0.001. (E) Reactivity is shown at the single cell level with the induction of significant proportions of degranulating CD107a<sup>+</sup> and IFN $\gamma$ <sup>+</sup> NK cells upon short-term stimulation with K562 target cells in a representative FCM dot-plot.

HSPC-NK released substantial amounts of these factors upon culture with all three OC cell lines (Fig. 2B and C). Notably, the levels of IFN $\gamma$  and GzmB released by HSPC-NK cells against SKOV-3 cells were lower than with the other OC cell lines. This was also in line with the relatively lower killing susceptibility of SKOV-3 cells by HSPC-NK cells compared with IGROV1 and OVCAR-3. To investigate whether this is related to the expression of certain activating NK-ligands, we performed FCM analysis of the used OC cell lines and compared them with EpCAM<sup>+</sup> OC cells in ascites samples

of 10 different patients. This analysis showed that OC cell lines and patient's OC cells in ascites have similar levels of the NK-activating ligands including MICA/B, ULBP-1, ULBP-2, DNAM1 ligands (CD112, CD155) and TRAIL receptors (Fig. 2D and E). Together these data demonstrate that OC cells display expression of NK-activating ligands and are highly susceptible to killing by SR1/IL-15/IL-12 induced HSPC-NK cells. From these data, we have chosen SKOV-3 with the lowest NK-sensitivity as a clinically relevant model for further studies.

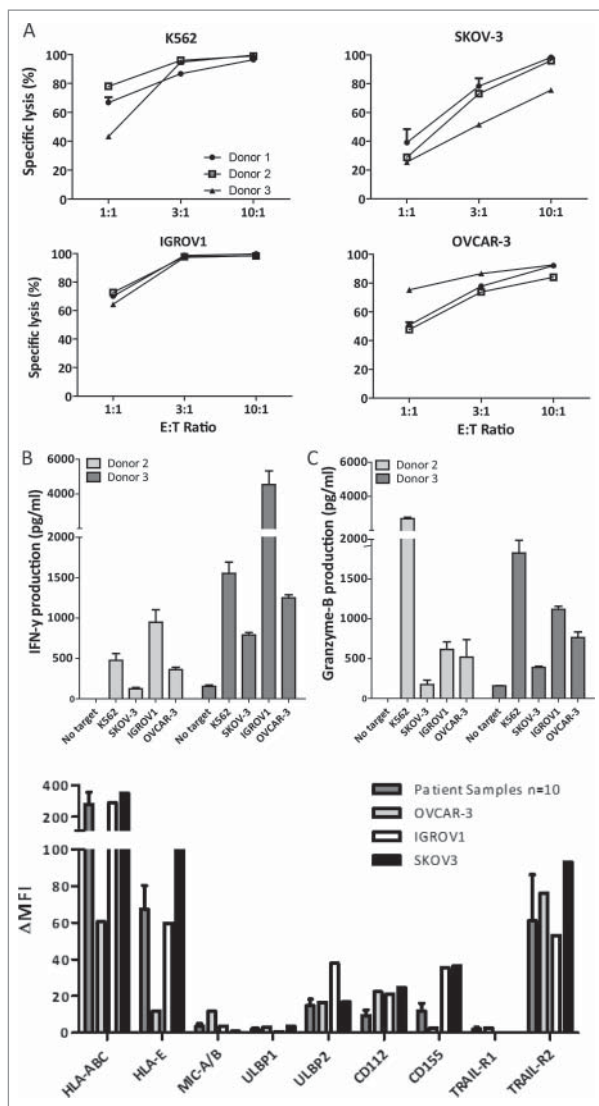


**Figure 2.** HSPC-NK cells are effective killers of ovarian cancer cell monolayers. (A) Percentage of specific lysis after 24 h co-culture of HSPC-NK cells with different OC cell lines. Graphs represent data of three different UCB-donors. (B) IFN $\gamma$  production by HSPC-NK cells from different donors against OC cell lines after 24 h co-culture. (C) Release of Granzyme-B by HSPC-NK cells against OC cell lines after 24 h co-culture. Graphs represent the mean  $\pm$  SEM of three experiments. (D) Delta of mean fluorescence index of NK-activation markers of SKOV-3 cells vs. tumor cells (EPCAM $^{+}$ ) of 10 patient ascites samples. Data of EPCAM $^{+}$  tumor cells of 10 patients are depicted as the mean  $\pm$  SEM.

### Ovarian carcinoma spheroids are effectively infiltrated and attacked by HSPC-NK cells

To investigate the potency of HSPC-NK cells to infiltrate and kill OC cells in a more physiologic assay for OC deposits, we set up an OC spheroid culture system using SKOV-3 cells (Fig. 3A). Plating of SKOV-3 cells in agarose-coated plates resulted in the formation of well-defined spheroids within 72 h (Fig. 3B and C), which were used to test HSPC-NK cell killing and infiltration capacity. After overnight incubation (18 h), NK cell clustering around the spheres was evident and addition of higher NK cell numbers resulted in disruption of the spheroids (Fig. 3C). Accordingly, FCM analysis of the co-cultures after 24 h confirmed a dose response relationship between the amount of NK cells added and the percentage killing of OC

cells, resulting in to >90% target cell killing after co-culture with  $2 \times 10^6$  HSPC-NK cells (Fig. 3D). Furthermore, HSPC-NK cells significantly secreted IFN $\gamma$  and Granzyme-B upon co-culture with SKOV-3 spheroids (Fig. 3E and F).

Next, we studied whether lysis of OC cells by HSPC-NK cells occurred primarily from the outside or also within the core of the spheroids. To address this, we examined NK cell infiltration in time by FCM and confocal microscopy. First, we performed an FCM-based infiltration assay and showed that about one-third of the added HSPC-NK cells infiltrate into the spheroid, which was similar after co-culture with different amounts of HSPC-NK cells (Fig. S1). This observation indicates that at higher HSPC-NK cell numbers, more NK cells will invade into the tumor spheroids resulting in higher intratumoral killing and destruction. Following a more extensive washing protocol to exclude the disrupted outer part of the spheroid, we demonstrated progressive infiltration of the spheroids by HSPC-NK cells peaking at 8 h (Fig. 4A). After 24 h, less infiltrating NK cells were detected, likely due to disruption of the spheroid as a consequence of HSPC-NK cell-mediated tumor cell killing.

To demonstrate that the infiltrated HSPC-NK cells actually kill SKOV-3 cells inside the spheroid, we collected and washed the co-cultured spheroids after 5 h, and transferred them to a new well for an overnight killing assay, thus without NK cells in the supernatant. Notably, after initial administration of  $2 \times 10^5$  HSPC-NK cells, no killing was measured (Fig. 4B). However, at higher E:T ratios with  $6 \times 10^5$  HSPC-NK cells >50% of SKOV-3 target cells were killed by the infiltrated HSPC-NK cells. To further visualize HSPC-NK cell infiltration into the multicellular SKOV-3 spheroid, we performed time-lapse imaging with confocal microscopy. Already after 1 h of co-culture, infiltrating and migrating CD56 $^{+}$  cells were observed in the outer third of the 500  $\mu$ m diameter sphere. Gradually, HSPC-NK cell numbers increased in the outer area, while migrating NK cells reached the core of the sphere after 5 h of co-culture (Fig. 4C). Time-lapse movies demonstrated that HSPC-NK cells actively migrate into the SKOV-3 spheroid and mediate killing inside the spheroid (Video S1 and S2).

Quantification by using the propidium iodide (PtdIns) signal during co-culture showed that dead SKOV-3 cells were found in the outer 5–15  $\mu$ m of the spheroid, but SKOV-3 cell death was also significantly observed up to 60  $\mu$ m within the spheroid (i.e., detection limit confocal microscopy;  $p < 0.0001$  compared with untreated spheres; Fig. 4D). At 5 h, the amount of PtdIns-positive cells per nm $^2$  increased 12 times from 5 to 60, while in the untreated SKOV spheres the amount only doubled (Fig. 4E and F). Collectively, these data demonstrate that HSPC-NK cells efficiently migrate, infiltrate, and mediate intratumoral killing of OC cells in a tumor spheroid.

### Intraperitoneally transfused HSPC-NK cells inhibits OC progression in vivo

Based on the encouraging data, we obtained *in vitro* on HSPC-NK cell mediated killing of OC cells and spheres, and we next aimed at evaluating the antitumor potential of HSPC-NK cells *in vivo*. To achieve this, we established an OC mouse model by i.p. inoculation of luciferase-expressing SKOV-3 cells into NSG mice (Fig. 5A). This model resulted



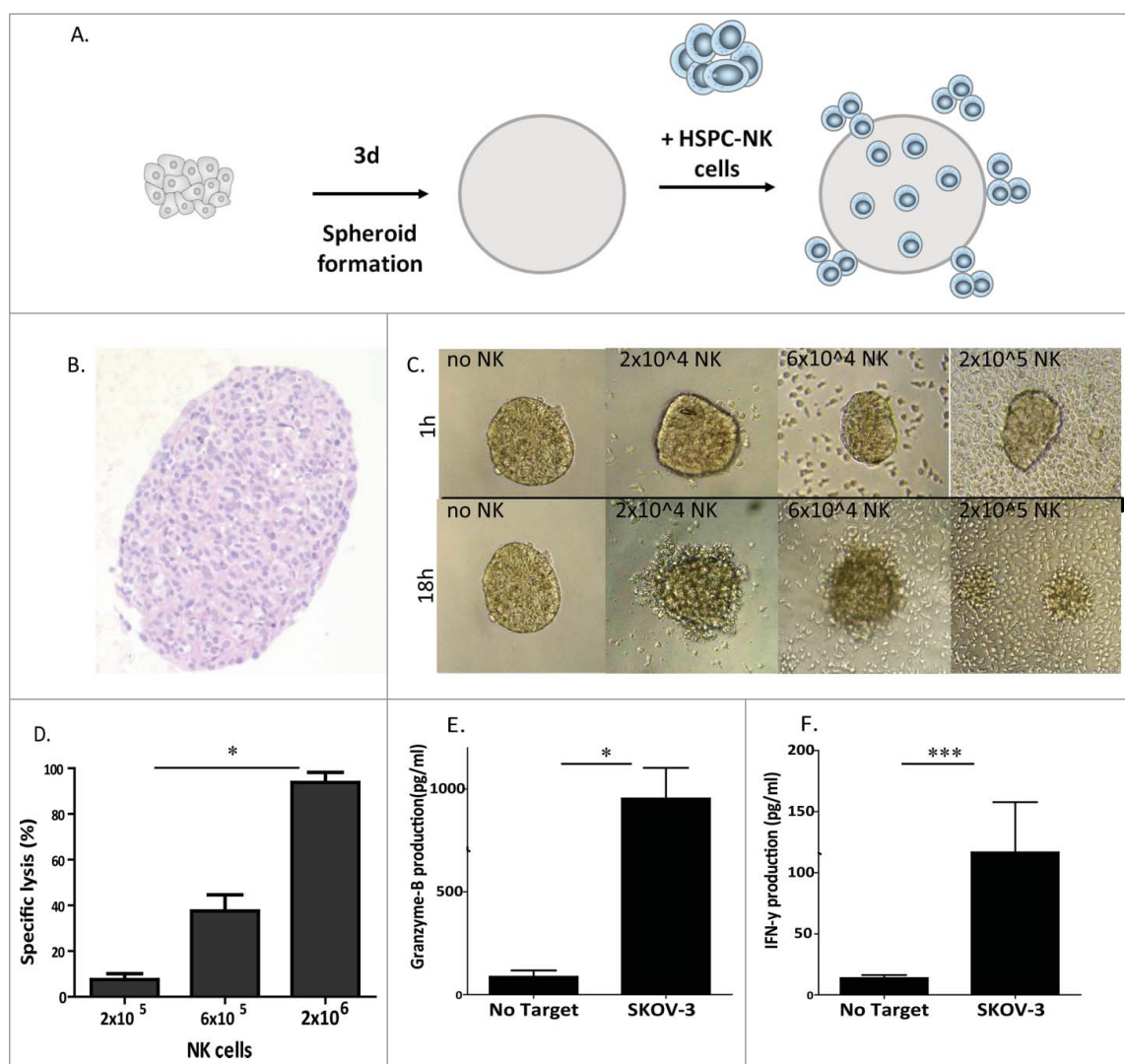


**Figure 3.** HSPC-NK cells have high cytolytic activity against SKOV-3 spheroids. (A) Experimental design illustrating the formation of SKOV-3 spheroids, NK cell transfer, and different functional assays performed. (B) H&E staining at 72 h on  $4 \mu\text{m}$  thick section of the SKOV-3 spheroid. (C) Overview of SKOV-3 spheroid co-cultures without (i.e., medium control) and with  $2 \times 10^4$ ,  $6 \times 10^4$ , and  $20 \times 10^4$  HSPC-NK cells. Pictures by light microscopy were taken after 1 h co-culture (top panel) and after 18 h co-culture (bottom panel). (D) Specific lysis by HSPC NK cells of SKOV-3 tumor cells within the spheroids at different E:T ratios. Data are shown as mean  $\pm$  SEM of a three experiment. Two-way ANOVA  $p = 0.02$  (E) and (F) GzmB and IFN $\gamma$  production of HSPC-NK cells after 24 h co-culture with SKOV-3 spheroids (unpaired t-test IFN $\gamma$   $p = 0.04$ , GzmB  $p = 0.0009$ ).

in SKOV-3 tumor development in ovaries and omentum, as well as small nodules deposition along the peritoneum (data not shown). Proliferation of SKOV-3 tumor cells in the nodules was confirmed by Ki67 staining (Fig. 5B). Because one requirement for ACT is the homing of the infused cells to the tumor site, we tested the effect of HSPC-NK cells infused directly into the peritoneal cavity, the compartment where OC is located. Subsequently, tumor growth was analyzed by bioluminescence imaging (BLI). In a first experiment, we observed a slight but significant reduction of SKOV-3 cell progression in mice receiving two HSPC-NK cell injections and IL-15 support till day 28 (Fig. 5C). Next, we performed a second experiment using a less stringent model by decreasing the number of SKOV-3 cells injected by 5-fold to  $0.2 \times 10^6$ . Here, the effect of HSPC-NK cells was more pronounced. Weekly measurement of the BLI signal indicated potent control of SKOV-3 cell progression by HSPC-NK cells (Fig. 5D). Importantly, these mice had

improved survival as compared with untreated mice (Fig. 5E). Furthermore, at sacrifice at day 92, the HSPC-NK-treated mice had a significant lower macroscopic tumor score on peritoneal surfaces. These results demonstrate that HSPC-NK cells are functional following i.p. infusion and able to efficiently target OC depositions *in vivo*.

## Discussion

The overall survival of patients diagnosed with recurrent and advanced stage ovarian carcinoma has only slightly improved in the last 20 y despite evolving therapies, illustrating the unmet need for new treatment modalities.<sup>1</sup> Since HLA class I molecules are often downregulated in ovarian carcinoma and evidence is emerging that OC cells are susceptible to NK cell-mediated cytotoxicity,<sup>27-29</sup> ACT exploiting allogeneic NK cells can be proposed as a prime candidate and relatively non-toxic treatment approach for OC patients. Previous studies have

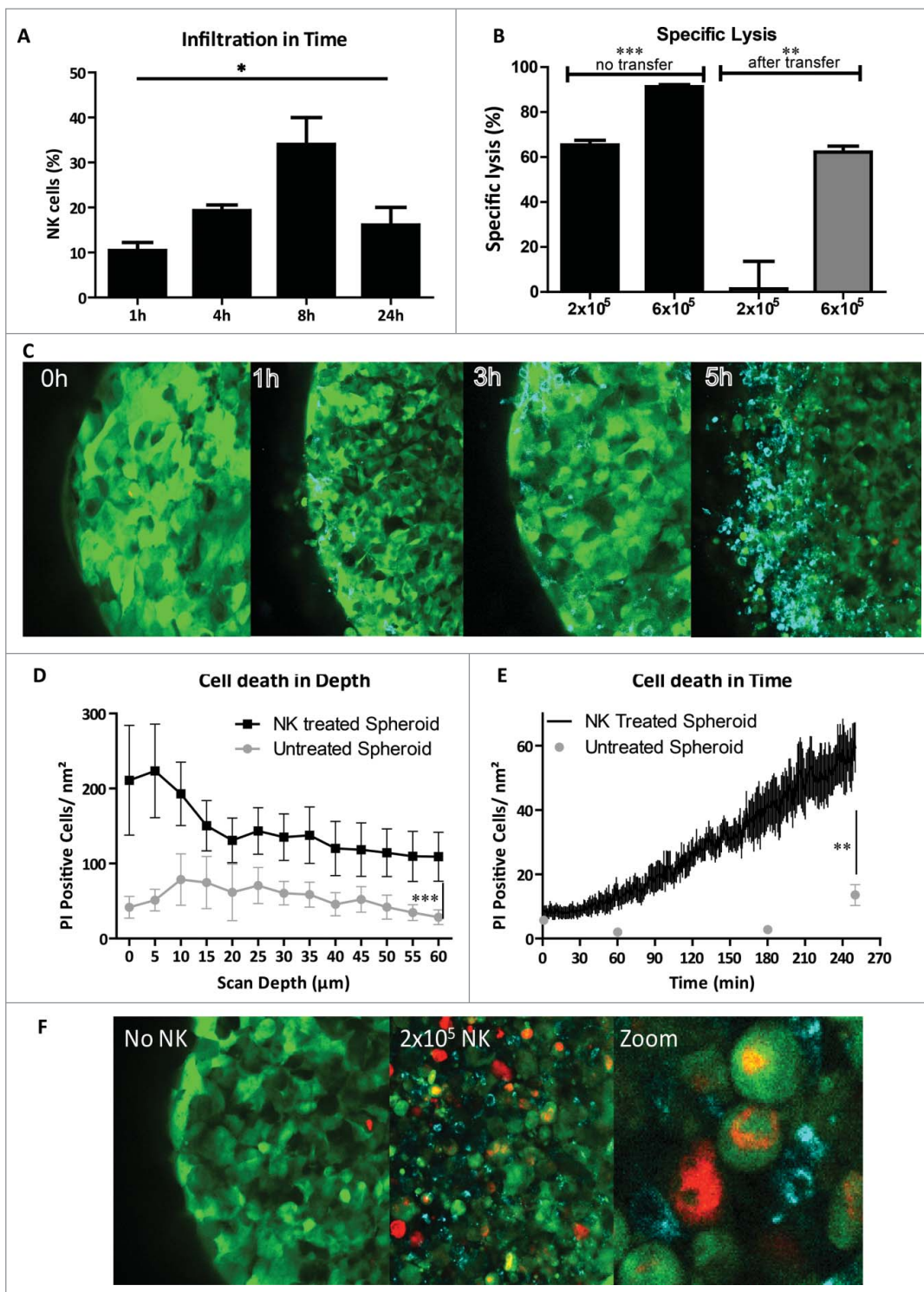


**Figure 4.** HSPC-NK cells infiltrate and mediate efficient intratumoral killing in SKOV-3 spheroids. (A) Percentage of infiltrated NK cells in SKOV-3 spheroids was measured by FCM after co-culture with  $2 \times 10^5$  NK cells and trypsinization on four different time points. Bars represent mean  $\pm$  SEM of four experiments. Two-way ANOVA  $p = 0.018$  (B) spheroids with infiltrated HSPC-NK cells after 5 h of incubation were transferred to a new well to measure the cytotoxic capacity of the infiltrated HSPC-NK cells. On the left, the percentage specific lysis without transfer is shown, and on the right, the specific HSPC-NK cell mediated lysis is depicted after 24 h incubation following transfer to a new well. Unpaired  $t$ -test comparing different HSPC-NK cell dosages without transfer shows a  $p$ -value of 0.0003, and a  $p$ -value of 0.008 comparing the transferred spheroids. (C) Confocal images of an SKOV-3 spheroid incubated with HSPC-NK cells after four time points. The green cells are GFP+ SKOV-3 cells and the blue cells are HSPC-NK cells infiltrating in the spheroid. (D) Amount of PtdIns positive SKOV-3 cells in the spheroids following incubation with HSPC-NK cells (in black), and in untreated spheroids (in gray), per scan depth in  $\mu\text{m}$ . Data are shown as mean  $\pm$  SD of a representative experiment. 60  $\mu\text{m}$  is the maximum scan depth for the used confocal microscopy. In the NK-treated spheres, the amount of PtdIns+ cells is significantly higher (two-way ANOVA;  $p < 0.0001$ ). (E) Amount of PtdIns positive SKOV-3 cells in time within HSPC-NK cell treated spheroid was calculated with the assistance of Fiji image analysis (in black). As control three time points of an untreated SKOV-3 spheroid is depicted in gray. SKOV-3 cell death is significantly increased within the HSPC-NK cell treated spheroid compared with untreated spheroid (unpaired  $t$ -test with the Welch correction;  $p = 0.004$ ). (F) Confocal image of SKOV-3 spheroid incubated 5 h with HSPC-NK cells, with addition of PtdIns. On the left, a spheroid without NK addition is shown, where few PtdIns positive cells are seen, in the middle a spheroid with HSPC-NK cells, where we see more dead cells, and on the left, a zoomed in picture of a part of the spheroid illustrating the infiltration of HSPC-NK cells causing cell death in an SKOV-3 spheroid.

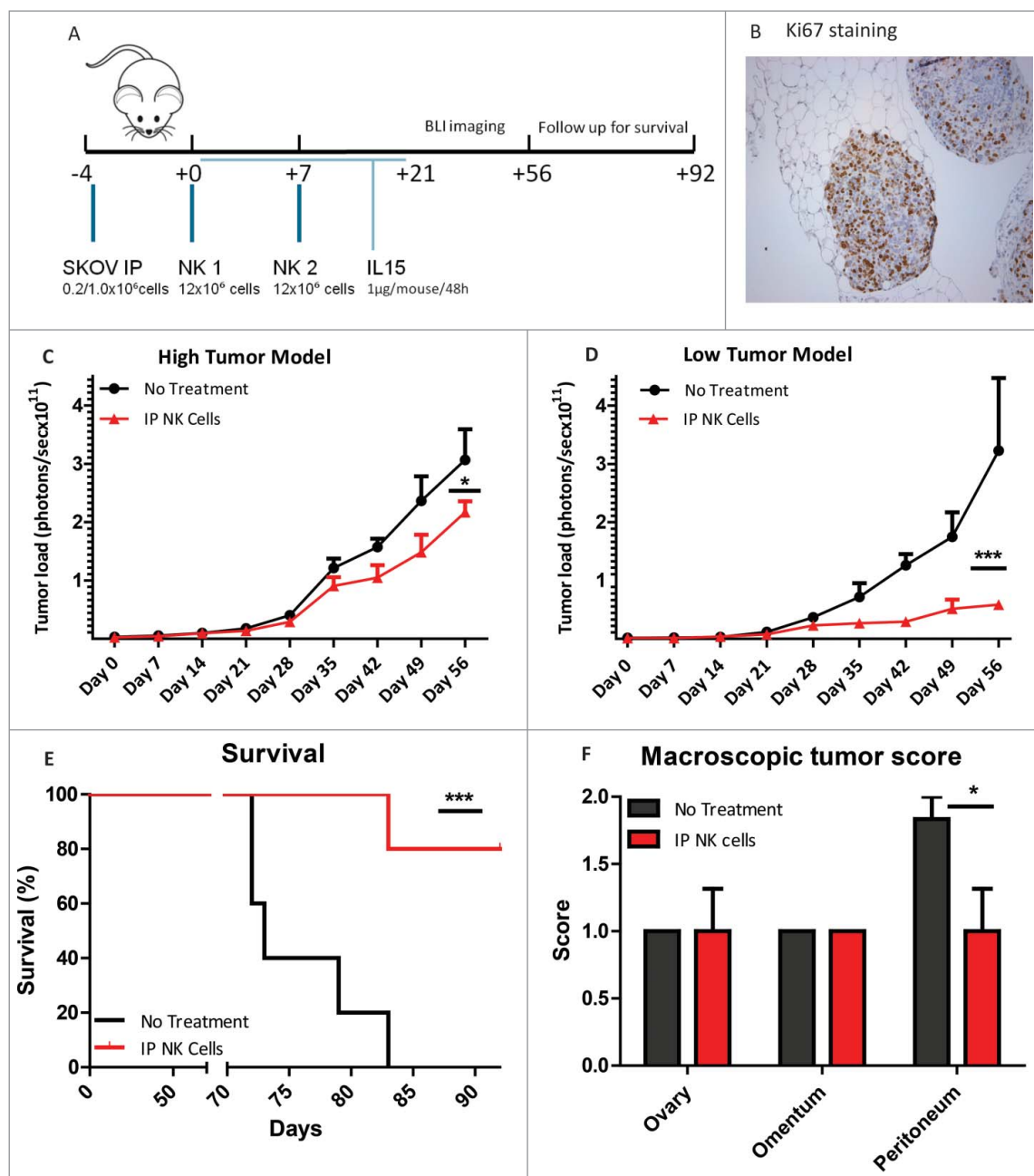


**Figure 5.** Intraoperative infusion of HSPC-NK cells slows down tumor growth and improves survival of OC-bearing NSG mice. (A) Experimental design of i.p. SKOV-3 injection and subsequent adoptive transfer of two HSPC-NK cell infusions combined with rhIL-15 administration till day 21. Tumor load was followed by BLI imaging till day 56 and mice were followed for survival till day 92. (B) Ki67 immunohistochemical staining of intraoperative SKOV-3 tumor nodules of NSG mice bearing SKOV-3 tumors, showing high tumor cell proliferation. (C) Results of the high tumor ( $1 \times 10^6$  SKOV-3 cells i.p.) dose experiment of the tumor size evaluation by the quantification of the bioluminescent signal (in photons per second per  $\text{cm}^2$ ) in a standardized ROI. In red, the BLI signal of mice treated with intraoperative HSPC-NK infusions and in black the untreated mice. HSPC-NK cell treatment significantly reduced tumor growth (two-way ANOVA;  $p = 0.016$ ). (D) Radiance in photons per second per  $\text{cm}^2$  of the lower tumor dose experiment with  $0.2 \times 10^6$  SKOV-3 cells i.p. HSPC-NK cell treatment significantly reduced tumor growth at this lower tumor burden (two-way ANOVA  $p = 0.0007$ ). (E) Percentage survival of the NSG mice of the low tumor dose experiment. Kaplan meier with the log rank Mantel Cox test showed a significance of  $p = 0.023$  and a hazard ratio of 6. (F) Macroscopic tumor score of the NSG mice after sacrificing at day 92 with a significantly lower tumor score on peritoneal surfaces after HSPC-NK cell treatment (Paired  $t$ -test;  $p = 0.034$ ).

shown that allogeneic NK cells rapidly recognize and destroy malignantly transformed OC cells *in vitro* and *in vivo*.<sup>2,3,21,22,30,31</sup> Here, we demonstrate that highly functional HSPC-NK cells generated by an optimized SR1/IL-15/IL-12-based expansion protocol are very potent killers of OC cells in relevant preclinical models. Moreover, we provide novel evidence that HSPC-NK cells are able to efficiently infiltrate, migrate, and mediate intratumoral killing of OC cells in a multicellular tumor spheroid and that after i.p. infusion HSPC-NK

cells slows down tumor progression and prolongs survival in OC-bearing mice.

Collectively, these findings provide a strong rationale for intraoperative HSPC-NK cell-based therapy against OC. To generate high numbers of allogeneic NK cells completely devoid of T cell contamination, we developed a GMP-compliant, cytokine-based, feeder-free *ex vivo* culture protocols. Using this procedure, CD34+ HSPCs isolated from widely available UCB units can be expanded over 1,000-fold into a mixture of

immature and mature NK cells with a purity of > 90%. In this study, we combined two recent optimizations, which include the AhR antagonist SR1 for improving NK cell differentiation, and the combination of IL-15 and IL-12 that stimulates the differentiation of more “memory-like” NK cells with a superior cytolytic and IFN $\gamma$  response upon target cell encounter.<sup>9,10</sup> This SR1/IL-15/IL-12 generated HSPC-NK cell product is even more pure; >90% and a total dosage up to  $3 \times 10^9$  HSPC-NK cells for i.p. infusion in OC patients can be readily generated from a single HSPC donor. This is a higher purity and yield than NK products from other sources and protocols.<sup>4-6,32,33</sup>

These highly active HSPC-NK cells rapidly recognize and destroy malignantly transformed cells *in vitro* when added to tumor cell monolayers. Although tumor monolayer cell culture is traditionally used,<sup>2,3,17,33,34</sup> it neglects the 3D tumor structure, thereby potentially overestimating the translation to the *in vivo* situation. Therefore, 3D tumor spheroid models have been developed to better investigate solid tumor-NK cell interactions, and more closely resemble the tumor microenvironment than conventional monolayer cultures. These multicellular tumor spheroids are formed by the association of several thousands of cells and consist of an outer rim of proliferating cells around a core of quiescent tumor cells.<sup>14</sup> So far, a few studies are published using tumor spheroids to assess NK cell infiltration and intratumoral cytotoxicity dynamics. Giannattasio et al. showed that IL-2 pre-activated and expanded PB-NK cells can invade cervical cancer spheroids.<sup>15</sup> We have adopted the spheroid system of Giannattasio et al. and showed by real-time monitoring that infiltrated HSPC-NK cells in OC spheroids mediate efficient intratumoral killing, which is of clinical relevance for HSPC-NK cell therapy in OC treatment. However, still many questions remain unanswered about the mechanism of action of activated NK cells in solid tumors. Furthermore, previous studies showed that 3D tumor spheroids are useful tools to study the stimulatory potential of other drugs and cells of the tumor microenvironment on NK cell function. For instance, inhibition of NK cell function in Ewing's sarcoma spheroids<sup>23</sup> and head and neck squamous cell carcinoma (HNSCC) spheroids<sup>16</sup> was reported. Interestingly, cetuximab, an anti-epidermal growth factor receptor (HER1) antibody, reconstituted pro-inflammatory cytokine secretion and tumor-infiltrating capacity of sMICA-inhibited NK cells in HNSCC spheroids.<sup>16</sup> In addition, Herter et al. recently used a 3D spheroid model composed of tumor cells, fibroblast, and immune cells to study the effect of combined treatment with a novel IgG-IL2v compound and tumor-targeting bispecific antibody.<sup>35</sup> Finally, we and Giannattasio et al. show that efficient tumor spheroid infiltration is performed by only a fraction of the activated NK cells. This could be related to differential phenotypes of infiltrating and non-infiltrating NK cells. Moreover, although some activated NK cells can kill up to 14 adjacent tumor cells within 6 h, each NK cell within a bulk population or product is not equally active in forming contacts and serial killing properties.<sup>17,18</sup> Therefore, further studies are warranted to decipher the behavior of individual HSPC-NK cells in different models; looking at infiltration in 3D tumor spheroids or even at *in vivo* behavior in intravital multiphoton microscopy in adoptive transfer studies in OC-bearing mice.<sup>36</sup>

Regarding the potency of HSPC-NK cells to target OC *in vivo*, we observed that two i.p. infusions plus IL-15 support inhibited tumor growth prolonged survival and resulted in a lower macroscopic tumor score in SKOV-3 bearing NSG mice. The localization of tumor depositions in the SKOV-3 tumor xenograft model in omentum, ovaries, and peritoneal surfaces makes the model clinically relevant. Through intraperitoneal infusion of highly active HSPC-NK cells, direct targeting of the tumor cells is facilitated. Important is the effect that is shown on the peritoneal surfaces, since omentum and ovaries are removed during surgery. Tumor depositions on the peritoneum are difficult to resect, often causing incomplete debulking and therefore important in prognosis of OC patients.

Good infiltration rates are considered a critical factor for effective adoptive NK cell therapy.<sup>37</sup> In a bladder cancer mouse model, intravesical NK cell administration shows a significant higher infiltration rate than systemic delivery.<sup>33</sup> Furthermore, investigators at the University of Minnesota have clearly demonstrated in a mouse model with the OC cell line MA148 that the i.p. delivery route of activated NK cells is superior to i.v. infusion for an effective anti-OC effect.<sup>2,3</sup> Previously, we and others have observed that a large proportion of activated NK cells are trapped in the liver upon i.v. infusion,<sup>13,38,39</sup> and therefore i.p. infusion of a high dose of HSPC-NK cells can immediately attack the OC cells as NK sequestration in the liver will be prevented.

Although we have observed significant anti-OC effects of HSPC-NK cells in SKOV-3 tumor spheroids and xenograft models, potentiating of the anti-OC reactivity *in vivo* might be needed in patients. Different strategies to improve HSPC-NK cell-ACT could be explored. For instance, combining HSPC-NK cell infusion with i.p. administration of the IL-15 superagonist ALT-803 might be promising. ALT-803 has a longer half-life than rhIL-15 and represents an effective IL-15 receptor-agonist that augments NK cell proliferation, cytotoxic potential and antibody-dependent cell-mediated cytotoxicity (ADCC).<sup>19</sup> Other factors that might enhance the anti-OC effect are to be investigated, especially combination therapy with tumor-targeting antibodies or immune modulatory agents seems promising. ADCC is attractive because of the rapidly upregulated CD16 expression of our HSPC-NK cell product *in vivo* and cytotoxic anti-OC activity could be enhanced with a targeted antibody.<sup>9</sup> Similar to cytotoxic T cells, chimeric antigen receptor-mediated antitumor activity has been demonstrated using different NK cell sources and might provide a method to redirect these cells more specifically to target refractory cancers.<sup>34</sup> Another option to improve HSPC-NK cell therapy is to sensitize tumor cells to NK cell mediated killing by combined treatment with hypomethylating agents such as decitabine.<sup>40</sup>

In conclusion, our data strongly support that SR1/IL-15/IL12 expanded HSPC-NK cells constitute a promising immunotherapeutic product that can be exploited for intraperitoneal therapy of OC patients, as demonstrated by their capability to actively migrate, infiltrate, and mediate intratumoral cell killing in OC spheroids. In addition, we demonstrated promising pre-clinical anti-OC activity of HSPC-NK cells following intraperitoneal infusion in a relevant SKOV-3-based OC xenograft model. Finally, the methodologies reported here to study HSPC-NK cell infiltration capacity and anti-OC effects will be

instrumental to validate future combination therapies for the treatment of refractory or relapsed OC patients.

## Disclosure of potential conflicts of interest

No potential conflicts of interest were disclosed.

## Acknowledgments

The authors thank all patients for giving consent for usage of their ascites material. We would like to thank the team of the Radboudumc Central Animal Laboratory and all colleagues from the Laboratory of Hematology for kind assistance and constructive discussion on this project.

## Funding

This work was supported by grants from the Radboudumc and the Dutch Cancer Society (KWF: KUN 2015-7507).

## Author contributions

JSH designed research, performed experiments, analyzed data, and wrote the manuscript; JC designed research, performed experiments and analyzed data; DB designed research, performed experiments and analyzed data; MO performed experiments; RB, RT, RLB, JJ, LM provided advice and reviewed manuscript; HD designed and supervised research and wrote the manuscript.

## References

- Siegel RL, Miller KD, Jemal A. Cancer statistics, 2015. *CA Cancer J Clin* 2015; 65(1):5-29; PMID:25559415; <https://doi.org/10.3322/caac.21254>
- Geller MA, Knorr DA, Hermanson DA, Pribyl L, Bendzick L, McCullar V, Miller JS, Kaufman DS. Intraperitoneal delivery of human natural killer cells for treatment of ovarian cancer in a mouse xenograft model. *Cytotherapy* 2013; 15(10):1297-306; PMID:23993303; <https://doi.org/10.1016/j.jcyt.2013.05.022>
- Hermanson DL, Bendzick L, Pribyl L, McCullar V, Vogel RI, Miller JS, Geller MA, Kaufman DS. Induced pluripotent stem cell-derived natural killer cells for treatment of ovarian cancer. *Stem Cells* 2016; 34(1):93-101; PMID:26503833; <https://doi.org/10.1002/stem.2230>
- Davis ZB, Felices M, Verneris MR, Miller JS. Natural killer cell adoptive transfer therapy: Exploiting the first line of defense against cancer. *Cancer J* 2015; 21(6):486-491; PMID:26588681; <https://doi.org/10.1097/PPO.0000000000000156>
- Miller JS, Soignier Y, Panoskaltis-Mortari A, McNearney SA, Yun GH, Fautsch SK, McKenna D, Le C, Defor TE, Burns LJ et al. Successful adoptive transfer and *in vivo* expansion of human haploidentical NK cells in patients with cancer. *Blood* 2005; 105(8):3051-7; PMID:15632206; <https://doi.org/10.1182/blood-2004-07-2974>
- Geller MA, Cooley S, Judson PL, Ghebre R, Carson LF, Argenta PA, Jonson AL, Panoskaltis-Mortari A, Curtsinger J, McKenna D et al. A phase II study of allogeneic natural killer cell therapy to treat patients with recurrent ovarian and breast cancer. *Cytotherapy* 2011; 13(1):98-107; PMID:20849361; <https://doi.org/10.3109/14653249.2010.515582>
- Bachanova V, Cooley S, Defor TE, Verneris MR, Zhang B, McKenna DH, Curtsinger J, Panoskaltis-Mortari A, Lewis D, Hippen K et al. Clearance of acute myeloid leukemia by haploidentical natural killer cells is improved using IL-2 diphtheria toxin fusion protein. *Blood* 2014; 123(25):3855-63; PMID:24719405; <https://doi.org/10.1182/blood-2013-10-532531>
- Sachamitr P, Hackett S, Fairchild PJ. Induced pluripotent stem cells: Challenges and opportunities for cancer immunotherapy. *Front Immunol* 2014; 5:176; PMID:24860566; <https://doi.org/10.3389/fimmu.2014.00176>
- Cany J, van der Waart AB, Spanholtz J, Tordoir M, Jansen JH, van der Voort R, Schaap NM, Dolstra H. Combined IL-15 and IL-12 drives the generation of CD34-derived natural killer cells with superior maturation and alloreactivity potential following adoptive transfer. *Oncoimmunology* 2015; 4(7):e1017701; PMID:26140247; <https://doi.org/10.1080/2162402X.2015.1017701>
- Roeven MW, Thordardottir S, Kohela A, Maas F, Preijers F, Jansen JH, Blijlevens NM, Cany J, Schaap N, Dolstra H. The aryl hydrocarbon receptor antagonist StemRegenin1 improves *in vitro* generation of highly functional natural killer cells from CD34(+) hematopoietic stem and progenitor cells. *Stem Cells Dev* 2015; 24(24):2886-98; PMID:26414401; <https://doi.org/10.1089/scd.2014.0597>
- Spanholtz J, Preijers F, Tordoir M, Trilsbeek C, Paardekooper J, de Witte T, Schaap N, Dolstra H. Clinical-grade generation of active NK cells from cord blood hematopoietic progenitor cells for immunotherapy using a closed-system culture process. *PLoS One* 2011; 6(6):e20740; PMID:21698239; <https://doi.org/10.1371/journal.pone.0020740>
- Spanholtz J, Tordoir M, Eissens D, Preijers F, van der Meer A, Joosten I, Schaap N, de Witte TM, Dolstra H. High log-scale expansion of functional human natural killer cells from umbilical cord blood CD34-positive cells for adoptive cancer immunotherapy. *PLoS One* 2010; 5(2):e9221; PMID:20169160; <https://doi.org/10.1371/journal.pone.0009221>
- Cany J, van der Waart AB, Tordoir M, Franssen GM, Hangalapura BN, de Vries J, Boerman O, Schaap N, van der Voort R, Spanholtz J et al. Natural killer cells generated from cord blood hematopoietic progenitor cells efficiently target bone marrow-residing human leukemia cells in NOD/SCID/IL2Rg(null) mice. *PLoS One* 2013; 8(6):e64384; PMID:23755121; <https://doi.org/10.1371/journal.pone.0064384>
- Geller MA, Miller JS. Use of allogeneic NK cells for cancer immunotherapy. *Immunotherapy* 2011; 3(12):1445-59; PMID:22091681; <https://doi.org/10.2217/imt.11.131>
- Giannattasio A, Weil S, Kloess S, Ansari N, Stelzer EH, Cerwenka A, Steinle A, Koehl U, Koch J. Cytotoxicity and infiltration of human NK cells in *in vivo*-like tumor spheroids. *BMC Cancer* 2015; 15:351; PMID:25933805; <https://doi.org/10.1186/s12885-015-1321-y>
- Kloss S, Chambron N, Gardlowski T, Weil S, Koch J, Esser R, Pogge von Strandmann E, Morgan MA, Arseniev L, Seitz O, Kohl U. Cetuximab reconstitutes pro-inflammatory cytokine secretions and tumor-infiltrating capabilities of sMICA-Inhibited NK cells in HNSCC tumor spheroids. *Front Immunol* 2015; 6:543; PMID:26579120; <https://doi.org/10.3389/fimmu.2015.00543>
- Bhat R, Watzl C. Serial killing of tumor cells by human natural killer cells—enhancement by therapeutic antibodies. *PLoS One* 2007; 2(3):e326; PMID:17389917; <https://doi.org/10.1371/journal.pone.0000326>
- Choi PJ, Mitchison TJ. Imaging burst kinetics and spatial coordination during serial killing by single natural killer cells. *Proc Natl Acad Sci U S A* 2013; 110(16):6488-93; PMID:23576740; <https://doi.org/10.1073/pnas.1221312110>
- Rosario M, Liu B, Kong L, Collins LI, Schneider SE, Chen X, Han K, Jeng EK, Rhode PR, Leong JW et al. The IL-15-based ALT-803 complex enhances FcγRIIIa-triggered NK cell responses and *in vivo* clearance of B cell lymphomas. *Clin Cancer Res* 2016; 22(3):596-608; PMID:26423796; <https://doi.org/10.1158/1078-0432.CCR-15-1419>
- Ames E, Canter RJ, Grossenbacher SK, Mac S, Chen M, Smith RC, Hagino T, Perez-Cunningham J, Sckisel GD, Urayama S et al. NK cells preferentially target tumor cells with a cancer stem cell phenotype. *J Immunol* 2015; 195(8):4010-9; PMID:26363055; <https://doi.org/10.4049/jimmunol.1500447>
- Kozłowska AK, Kaur K, Topchyan P, Jewett A. Novel strategies to target cancer stem cells by NK cells; studies in humanized mice. *Front Biosci (Landmark Ed)* 2017; 22:370-84; PMID:27814619; <https://doi.org/10.2741/4489>
- Koh J, Lee SB, Park H, Lee HJ, Cho NH, Kim J. Susceptibility of CD24(+) ovarian cancer cells to anti-cancer drugs and natural killer cells. *Biochem Biophys Res Commun* 2012; 427(2):373-8; PMID:22995296; <https://doi.org/10.1016/j.bbrc.2012.09.067>
- Holmes TD, El-Sherbiny YM, Davison A, Clough SL, Blair GE, Cook GP. A human NK cell activation/inhibition threshold allows small

- changes in the target cell surface phenotype to dramatically alter susceptibility to NK cells. *J Immunol* 2011; 186(3):1538-45; PMID:21191066; <https://doi.org/10.4049/jimmunol.1000951>
24. Friedrich J, Seidel C, Ebner R, Kunz-Schughart LA. Spheroid-based drug screen: Considerations and practical approach. *Nat Protoc* 2009; 4(3):309-24; PMID:19214182; <https://doi.org/10.1038/nprot.2008.226>
  25. Schindelin J, Arganda-Carreras I, Frise E, Kaynig V, Longair M, Pietzsch T, Preibisch S, Rueden C, Saalfeld S, Schmid B et al. Fiji: An open-source platform for biological-image analysis. *Nat Methods* 2012; 9(7):676-82; PMID:22743772; <https://doi.org/10.1038/nmeth.2019>
  26. Taylor CR, Shi SR, Chaiwun B, Young L, Imam SA, Cote RJ. Strategies for improving the immunohistochemical staining of various intranuclear prognostic markers in formalin-paraffin sections: Androgen receptor, estrogen receptor, progesterone receptor, p53 protein, proliferating cell nuclear antigen, and Ki-67 antigen revealed by antigen retrieval techniques. *Hum Pathol* 1994; 25(3):263-70; PMID:7512074; [https://doi.org/10.1016/0046-8177\(94\)90198-8](https://doi.org/10.1016/0046-8177(94)90198-8)
  27. Norell H, Carlsten M, Ohlum T, Malmberg KJ, Masucci G, Schedvins K, Altermann W, Handke D, Atkins D, Seliger B et al. Frequent loss of HLA-A2 expression in metastasizing ovarian carcinomas associated with genomic haplotype loss and HLA-A2-restricted HER-2/neu-specific immunity. *Cancer Res* 2006; 66(12):6387-94; PMID:16778217; <https://doi.org/10.1158/0008-5472.CAN-06-0029>
  28. Vitale M, Pelusi G, Taroni B, Gobbi G, Micheloni C, Rezzani R, Donato F, Wang X, Ferrone S. HLA class I antigen down-regulation in primary ovary carcinoma lesions: Association with disease stage. *Clin Cancer Res* 2005; 11(1):67-72; PMID:15671529
  29. Gooden M, Lampen M, Jordanova ES, Leffers N, Trimbos JB, van der Burg SH, Nijman H, van Hall T. HLA-E expression by gynecological cancers restrains tumor-infiltrating CD8(+) T lymphocytes. *Proc Natl Acad Sci U S A* 2011; 108(26):10656-61; PMID:21670276; <https://doi.org/10.1073/pnas.1100354108>
  30. Cheng M, Ma J, Chen Y, Zhang J, Zhao W, Zhang J, Wei H, Ling B, Sun R, Tian Z. Establishment, characterization, and successful adaptive therapy against human tumors of NKG cell, a new human NK cell line. *Cell Transplant*. 2011; 20(11-12):1731-46; PMID:21669033; <https://doi.org/10.3727/096368911X580536>
  31. Jewett A, Man YG, Tseng HC. Dual functions of natural killer cells in selection and differentiation of stem cells; role in regulation of inflammation and regeneration of tissues. *J Cancer* 2013; 4(1):12-24; PMID:23386901; <https://doi.org/10.7150/jca.5519>
  32. Alves PC, Andrade LA, Petta CA, Lorand-Metze I, Derchain SF, Guimaraes F. Ex vivo expansion of CD56+ NK and NKT-like lymphocytes from peripheral blood mononuclear cells of patients with ovarian neoplasia. *Scand J Immunol* 2011; 74(3):244-52; PMID:21595734; <https://doi.org/10.1111/j.1365-3083.2011.02576.x>
  33. Ferreira-Teixeira M, Paiva-Oliveira D, Parada B, Alves V, Sousa V, Chijioke O, Munz C, Reis F, Rodrigues-Santos P, Gomes C. Natural killer cell-based adoptive immunotherapy eradicates and drives differentiation of chemoresistant bladder cancer stem-like cells. *BMC Med* 2016; 14(1):163; PMID:27769244; <https://doi.org/10.1186/s12916-016-0715-2>
  34. Hermanson DL, Kaufman DS. Utilizing chimeric antigen receptors to direct natural killer cell activity. *Front Immunol* 2015; 6:195; PMID:25972867; <https://doi.org/10.3389/fimmu.2015.00195>
  35. Herter S, Morra L, Schlenker R, Sulcova J, Fahrni L, Waldhauer I, Lehmann S, Reislender T, Agarkova I, Kelm JM et al. A novel three-dimensional heterotypic spheroid model for the assessment of the activity of cancer immunotherapy agents. *Cancer Immunol Immunother* 2017; 66(1): 129-40; <https://doi.org/10.1007/s00262-016-1927-1>
  36. Deguine J, Breart B, Lemaitre F, Di Santo JP, Bousso P. Intravital imaging reveals distinct dynamics for natural killer and CD8(+) T cells during tumor regression. *Immunity* 2010; 33(4):632-44; PMID:20951068; <https://doi.org/10.1016/j.immuni.2010.09.016>
  37. Pandey V, Oyer JL, Igarashi RY, Gitto SB, Copik AJ, Altomare DA. Anti-ovarian tumor response of donor peripheral blood mononuclear cells is due to infiltrating cytotoxic NK cells. *Oncotarget* 2016; 7(6):7318-28; PMID:26802025; <https://doi.org/10.18632/oncotarget.6939>
  38. Brand JM, Meller B, Von Hof K, Luhm J, Bahre M, Kirchner H, Frohn C. Kinetics and organ distribution of allogeneic natural killer lymphocytes transfused into patients suffering from renal cell carcinoma. *Stem Cells Dev* 2004; 13(3):307-14; PMID:15186726; <https://doi.org/10.1089/154732804323099235>
  39. Matera L, Galetto A, Bello M, Baiocco C, Chiappino I, Castellano G, Stacchini A, Satolli MA, Mele M, Sandrucci S et al. *In vivo* migration of labeled autologous natural killer cells to liver metastases in patients with colon carcinoma. *J Transl Med* 2006; 4:49; PMID:17105663; <https://doi.org/10.1186/1479-5876-4-49>
  40. Wang Y, Chen C, Dong F, Ma S, Xu J, Gong Y, Cheng H, Zhou Y, Cheng T, Hao S. NK cells play a significant role in immunosurveillance at the early stage of MLL-AF9 acute myeloid leukemia via CD226/CD155 interactions. *Sci China Life Sci* 2015; 58(12):1288-98; PMID:26588911; <https://doi.org/10.1007/s11427-015-4968-3>